

Kinetic Studies of OH Reactions with a Series of Ketones

S. Le Calvé, D. Hitier, G. Le Bras, and A. Mellouki*

Laboratoire de Combustion et Systèmes Réactifs, CNRS, and Université d'Orléans, 45071 Orléans Cedex 2, France

Received: January 22, 1998; In Final Form: March 30, 1998

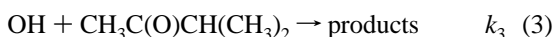
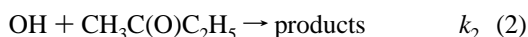
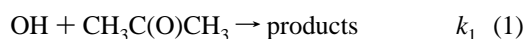
Absolute rate constants have been measured for the gas-phase reactions of hydroxyl radicals with a series of ketones: acetone (k_1), 2-butanone (k_2), 3-methyl 2-butanone (k_3), 4-methyl 2-pentanone (k_4), and 5-methyl 2-hexanone (k_5). Experiments were carried out using the pulsed laser photolysis–laser-induced fluorescence technique over the temperature range 243–372 K. The obtained kinetic data were used to derive the Arrhenius expressions: $k_1 = (1.25 \pm 0.22) \times 10^{-12} \exp[-(561 \pm 57)/T]$; $k_2 = (1.19 \pm 0.18) \times 10^{-12} \exp[-(60 \pm 61)/T]$; $k_3 = (1.58 \pm 0.35) \times 10^{-12} \exp[(193 \pm 65)/T]$; $k_4 = (0.759 \pm 0.126) \times 10^{-12} \exp[(834 \pm 46)/T]$, and $k_5 = (1.33 \pm 0.63) \times 10^{-12} \exp[(649 \pm 140)/T]$ (in units of $\text{cm}^3 \text{ molecule}^{-1} \text{ s}^{-1}$). At room temperature, the rate constants obtained (in units of $10^{-12} \text{ cm}^3 \text{ molecule}^{-1} \text{ s}^{-1}$) were as follows: acetone (0.184 ± 0.024); 2-butanone (1.19 ± 0.18); 3-methyl 2-butanone (2.87 ± 0.29); 4-methyl 2-pentanone (12.1 ± 0.9); and 5-methyl 2-hexanone (10.3 ± 1.0). Our results are compared with the previous determinations and discussed in terms of structure–reactivity relationships.

Introduction

Ketones are widely used as solvents in industry (paints, etc.), and a substantial proportion of these organic compounds (VOCs) can then escape to the atmosphere, where they become available for photochemical transformations. For example, 2-butanone, also known as methyl ethyl ketone (MEK), is rated tenth in the EPA's 1995 TRI (Toxics Release Inventory). With more than 70 million lbs released, it represents 3% of the total release in the TRI.¹ Ketones are also formed as intermediate products in the tropospheric chemical degradation of VOCs such as alkanes and alkenes.²

The atmospheric oxidation of these oxygenated VOCs, which is initiated by their tropospheric photolysis and reaction with the OH radical, may significantly contribute to the formation of ozone and other components of the photochemical smog in urban areas.

Kinetic and mechanistic information on OH-initiated oxidation is therefore needed to assess the impact of these VOCs on air quality. In this work, we report absolute rate constant data for the reactions of the OH radical with five ketones: acetone (k_1), 2-butanone (k_2), 3-methyl 2-butanone (k_3), 4-methyl 2-pentanone (k_4), and 5-methyl 2-hexanone (k_5), in the temperature range 243–372 K:



The temperature dependences of the rate coefficients of the present study are the first to be reported for reactions 3, 4, and

5 and the second for reactions 1 and 2. We also report the first determination of the rate coefficient at room temperature for reactions 3 and 5. In addition to the study of the atmospheric behavior of these ketones, our work aimed at better defining the reactivity of ketones toward the hydroxyl radical.

Experimental Section

The apparatus and experimental techniques used have been described in detail previously^{3,4} and are briefly discussed here. The pulsed laser photolysis–laser-induced fluorescence (PLP–LIF) technique was used. Two sources were used to generate the OH radicals: photolysis of H_2O_2 at $\lambda = 248 \text{ nm}$ (KrF excimer laser) and photolysis of HONO at $\lambda = 351 \text{ nm}$ (XeF excimer laser). The concentration of the OH radicals was monitored at various reaction times ranging from ca. $10 \mu\text{s}$ to 10 ms by pulsed laser induced fluorescence. A Nd:YAG-pumped frequency-doubled dye laser was used to excite the OH radical at $\lambda = 282 \text{ nm}$, and fluorescence was detected by a photomultiplier, fitted with a 309 nm narrow band-pass filter. The output pulse from the photomultiplier was integrated for a preset period by a gated charge integrator. Typically the fluorescence signals from 10–15 different delay times from 100 probe laser shots were averaged to generate OH concentration–time profiles over at least three lifetimes. Ketone/ H_2O_2 or ketone/HONO mixtures in helium diluent were flowed slowly through the cell, so that each photolysis/probe sequence interrogated a fresh gas mixture and reaction products did not build up in the cell.

All experiments were carried out under pseudo-first-order conditions with $[\text{ketone}] \gg [\text{OH}]_0$, the initial concentration of OH being $[\text{OH}]_0 < 2 \times 10^{11} \text{ molecules cm}^{-3}$. The temporal profiles of $[\text{OH}]$, therefore, followed the pseudo-first-order rate law

$$[\text{OH}]_t = [\text{OH}]_0 e^{-k't} \quad \text{where} \quad k'_i = k_i[\text{X}_i] + k_0'$$

X_i refers to the ketone in reaction i ($i = 1-5$) and k_i is the rate coefficient for the reaction of OH with the ketone (i). The decay

* To whom correspondence should be addressed.

rate, k_0' , is the first-order OH decay rate in the absence of the ketone. The value of k_0' is essentially the sum of the reaction rate of OH with its precursor (H_2O_2 or HONO) and the diffusion rate of OH out of the detection zone. The concentrations of OH at various reaction times (delay between the photolysis pulses and the probe pulses) were determined by measuring the LIF signals at those delay times. Weighted (according to the signal-to-noise of the measured signal at the given time) least-squares analysis was used to fit the data to the above equation and extract the values of k_i' . The second-order rate coefficients (k_i) were obtained from the measured values of k' at various ketone concentrations.

The helium carrier gas (UHP certified to > 99.9995% (Alphagas)) was used without purification. The 50 wt % H_2O_2 solution obtained from Prolabo was concentrated by bubbling helium through the solution to remove water for several days prior to use and constantly during the course of the experiments. It was admitted into the reaction cell by passing a small flow of helium through a glass bubbler containing H_2O_2 . HONO was produced in situ by reacting NaNO_2 (0.1 M) with diluted H_2SO_4 (10%) contained in a stirred round-bottomed flask. The effluent from the flask was swept into the cell by a known flow of helium. Acetone (>99.5%), 4-methyl 2-pentanone (>99.5%), and 5-methyl 2-hexanone ($\geq 99\%$) were from Aldrich; 2-butanone (>99.5%) and 3-methyl 2-butanone ($\approx 99\%$) were from Fluka. These compounds were further purified by repeated freeze, pump, and thaw cycles and fractional distillation before use.

For the kinetic measurements, the studied ketones were premixed with helium in a 10 L glass light-tight bulb to form 1–23% mixtures at a total pressure of ≈ 800 Torr. All the gases flowed into the reactor through Teflon tubing. The gas mixture containing the ketone, the photolytic precursor (H_2O_2 or HONO), and the bath gas (approximately 100 Torr of helium) was flowed through the cell with a linear velocity ranging between 1 and 3 cm s^{-1} . The concentrations of the ketones were calculated from their mass flow rates, temperature, and pressure in the reaction cell. All flow rates were measured with mass flowmeters calibrated by measuring the rate of pressure increase in a known volume. The pressure in the cell was measured with a capacitance manometer connected at the cell entrance.

Results and Discussion

For the studied ketones, except acetone, the OH decay plots, $\ln[\text{OH}] = f(t)$, showed excellent linearity when H_2O_2 was used as the OH precursor. The experiments were, therefore, performed with this OH source for 2-butanone, 3-methyl 2-butanone, 4-methyl 2-pentanone, and 5-methyl 2-hexanone. In contrast, some complications arose with acetone using H_2O_2 as the source of OH. The OH decay plots in the presence of acetone were curved. The possible role of photodissociation products of acetone was then considered. The reported UV spectrum of acetone shows that this compound absorbs at $\lambda = 248$ nm ($\sigma = 2.12 \times 10^{-20}$ $\text{cm}^2 \text{molecule}^{-1}$). Using this value, we can calculate that under our experimental conditions up to 1×10^{12} molecules cm^{-3} of photoproducts could be produced in the photolysis cell. These photoproducts could be involved in secondary chemistry and explain the observed curvature. Nevertheless, while using a limited range of acetone concentration, we obtained a value for the rate constant close to that obtained when HONO was used as the OH source, but the data were somewhat scattered ($k_{298} = 1.9 \times 10^{-13}$ $\text{cm}^3 \text{molecule}^{-1} \text{s}^{-1}$). To avoid complications, we have performed the complete

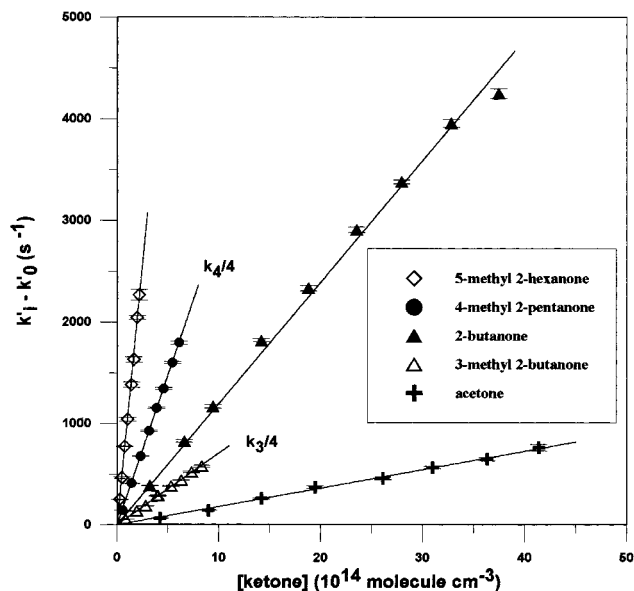


Figure 1. Plots of $(k_i' - k_0')$ through $(k_5' - k_0')$ vs ketone concentration at room temperature. The lines represent the linear least-squares fitting.

set of experiments for the OH + acetone reaction at the photolysis wavelength $\lambda = 351$ nm, where acetone does not absorb.⁵ As given in Table 1, the concentrations of the ketones used to determine k_2 , k_3 , k_4 , and k_5 were lower than that of acetone in k_1 determination (because reactions 2–5 were faster than reaction 1). Thus, the contribution of the photofragments to the overall decays of OH was negligible, and no complication was observed for the other ketones while using H_2O_2 as OH source.

Possible contributions to the measured rate constants from secondary reactions of OH with the radicals produced in reactions 1–5 were significantly reduced by using a high range (10^2 – 10^4) of $[\text{ketone}]/[\text{OH}]$ ratios which did not show any difference in measured k_i values. Rate constants were also shown to be independent of variations in the flow velocity ($v = 1$ – 3 cm/s) through the reactor or changes in the total pressure of the system ($P = 100$ – 300 Torr) or variations in the photolysis laser fluence ($E = 2$ – 12 mJ), at 248 or 351 nm. The concentrations of HONO and H_2O_2 were estimated from the decay rate with $[\text{ketone}] = 0$ ($[\text{HONO}] \approx 3 \times 10^{13}$ and $[\text{H}_2\text{O}_2] \approx 1 \times 10^{14}$, in molecules cm^{-3}). Figure 1 shows the plots of $k_i' - k_0'$ versus the ketone concentration obtained at room temperature for the different ketones, from where values of k_i were derived from the least-squares fit of the straight lines. The quoted errors for k_i determined in this work include 2σ from the least-squares analysis and the estimated systematic error 5% (due to uncertainties in measured concentrations).

The experimental conditions and the measured values of the rate coefficients k_1 – k_5 over the temperature range 243–372 K are listed in Table 1. k_1 – k_5 are also shown in Figure 2 in the conventional Arrhenius form ($k = Ae^{-E_a/RT}$). The Arrhenius parameters for k_1 – k_5 are given in Table 2, where the obtained data are summarized with those from previous studies.

Comparison with Previous Results. The present results can be compared with the literature data for k_1 , k_2 , and k_4 whereas the first determinations are reported for k_3 and k_5 . Our value of k_1 is in good agreement with the only one previous absolute measurement as a function of temperature.⁶ The room-temperature values of the two studies differ by 15%, but they agree within the uncertainty ranges. The other reported absolute measurement of k_1 at 298 K⁷ is also in agreement within the uncertainty ranges. Concerning the relative rate measurements,

TABLE 1: Reactions OH + Acetone (1), OH + 2-Butanone (2), OH + 3-Methyl 2-Butanone (3), OH + 4-Methyl 2-Pentanone (4), and OH + 5-Methyl 2-Hexanone (5): Summary of Experimental Conditions and Measured k_1 , k_2 , k_3 , k_4 , and k_5

T (K)	[acetone] (10^{14}) ^a	$10^{13} \times$ ($k_1 \pm 2\sigma$) ^b	[2-butanone] (10^{14}) ^a	$10^{12} \times$ ($k_2 \pm 2\sigma$) ^b	[3-methyl 2-butanone] (10^{14}) ^a	$10^{12} \times$ ($k_3 \pm 2\sigma$) ^b	[4-methyl 2-pentanone] (10^{14}) ^a	$10^{12} \times$ ($k_4 \pm 2\sigma$) ^b	[5-methyl 2-hexanone] (10^{14}) ^a	$10^{12} \times$ ($k_5 \pm 2\sigma$) ^b
243	5.95–55.49	1.32 ± 0.10	1.78–20.58	1.21 ± 0.05						
243			1.59–19.25	1.28 ± 0.08						
253	5.17–53.18	1.38 ± 0.06	1.78–19.82	1.20 ± 0.05	1.29–12.33	3.68 ± 0.15	0.37–3.59	21.3 ± 0.2		
253	8.20–66.07	1.41 ± 0.07^f					0.59–7.01	20.4 ± 0.4		
253							1.25–11.64	19.5 ± 3.3^e		
253							0.49–4.21	23.5 ± 0.8^b		
263			1.69–18.99	1.19 ± 0.05	0.99–9.40	3.26 ± 0.08	0.62–6.97	18.2 ± 0.2	0.24–2.31	17.0 ± 0.4
263					1.88–17.69	3.32 ± 0.17^d				
273	10.07–91.28	1.53 ± 0.10	1.62–18.02	1.19 ± 0.09	1.20–11.43	3.26 ± 0.08	0.33–3.79	16.2 ± 0.3	0.21–2.21	15.4 ± 0.9
273			3.67–41.42	1.22 ± 0.07^e						
283									0.25–2.34	13.8 ± 0.5
286									0.17–2.01	12.8 ± 0.3
291									0.25–2.27	13.3 ± 0.4
293									0.19–1.96	12.2 ± 0.3
298	4.21–41.39	1.83 ± 0.09	1.61–16.42	1.22 ± 0.10	0.85–8.31	2.85 ± 0.09	0.31–3.45	12.3 ± 0.1	0.25–2.18	10.3 ± 0.4
298	8.87–82.98	1.89 ± 0.12	1.64–16.50	1.18 ± 0.12	1.14–10.16	2.83 ± 0.13	0.29–3.41	12.2 ± 0.2	0.20–2.00	10.1 ± 0.5
298	7.69–65.57	1.87 ± 0.15	3.08–11.19	1.19 ± 0.06	0.81–8.13	2.94 ± 0.15^c	0.53–6.08	11.8 ± 0.3	0.24–2.49	10.4 ± 0.5^f
298	16.59–100.68	1.76 ± 0.14^d	3.23–32.80	$1.22 \pm 0.03^{c,e}$			1.02–9.91	11.9 ± 0.2^d		
298			1.92–30.69	1.12 ± 0.08^d			0.67–7.60	12.1 ± 0.3^e		
298			3.32–36.58	1.23 ± 0.05^e						
313			1.40–16.16	1.12 ± 0.11			0.31–3.29	10.6 ± 0.2		
323	8.22–68.10	2.03 ± 0.17			0.80–7.60	2.78 ± 0.11			0.21–2.05	9.77 ± 0.98
333			1.38–14.42	1.19 ± 0.09			0.28–2.96	9.06 ± 0.21		
333			2.68–32.73	1.28 ± 0.06^e			0.26–3.13	9.44 ± 0.29^g		
348	7.63–73.36	2.49 ± 0.23			0.80–8.82	2.74 ± 0.11			0.20–2.12	8.90 ± 0.26
353			1.30–14.47	1.19 ± 0.09			0.25–2.96	8.28 ± 0.14		
371										
372	7.14–59.69	2.88 ± 0.07	1.18–12.89	1.36 ± 0.10	0.72–6.71	2.79 ± 0.06	0.25–2.77	7.47 ± 0.20	0.21–1.99	8.25 ± 0.29
372	11.24–64.52	2.78 ± 0.24^e	2.57–29.20	1.39 ± 0.04^e	1.41–11.83	2.71 ± 0.10^e	0.41–4.68	7.67 ± 0.26	0.34–3.27	7.76 ± 0.21^e

^a Units of molecule cm^{-3} . ^b Units of $\text{cm}^3 \text{ molecule}^{-1} \text{ s}^{-1}$. ^c Variation of the photolysis laser fluence (decrease by a factor of 3). ^d Variation of flow velocity (decrease by a factor of 3). ^e Experiments carried out at 300 Torr. ^f Variation of the photolysis laser fluence (decrease by a factor of 2). ^g Variation of the photolysis laser fluence (decrease by a factor of 4). ^h Experiments carried out at 30 Torr.

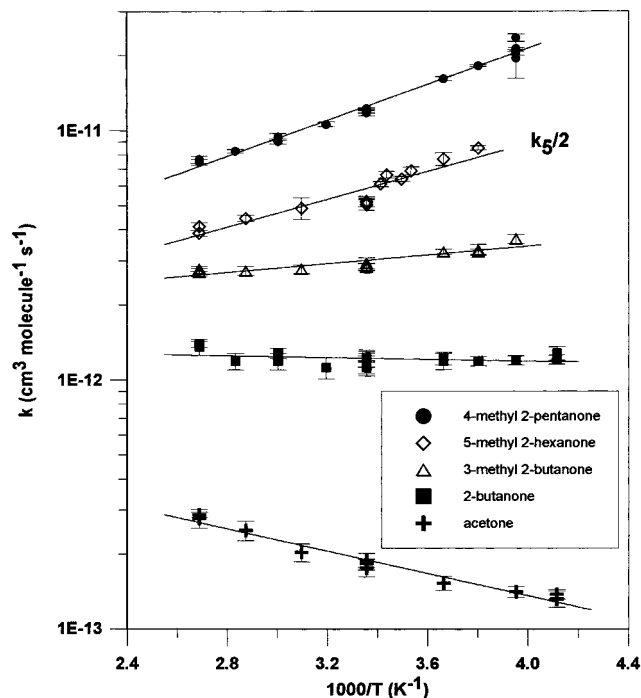


Figure 2. Plots of k_1 to k_5 vs $1/T$. The solid lines represent the Arrhenius parameter least-squares fits to the individual data points for each ketone. The error bars of the individual points are 2σ and do not include estimated systematic errors.

all performed at room temperature, the value of ref 8 is 47% higher than our determination. The k_1 value of ref 9 is 3.4 times higher and close to the upper limit of ref 10. In relative rate studies the precision might be limited by the use of a reference

reaction having a rate constant very different from k_1 . The OH + C_2H_4 reaction ($k = 8.1 \times 10^{-12} \text{ cm}^3 \text{ molecule}^{-1} \text{ s}^{-1}$ at 300 K and $P = 760 \text{ Torr}^{11}$) was used as the reference reaction in refs 10 and 8, and the reaction OH + n -hexane ($k = 5.9 \times 10^{-12} \text{ cm}^3 \text{ molecule}^{-1} \text{ s}^{-1}$ at 300 K¹¹) was used in ref 9. Finally, the present data fit well with the temperature-dependent expression of k_1 ,¹¹ recommended from the studies of refs 6, 8, and 12.

For the reaction of OH with 2-butanone, our value of k_2 is, as for k_1 , in excellent agreement with the only other temperature-dependent absolute determination of ref 6. Our value of k_2 also agrees fairly well with other room-temperature measurements obtained by an absolute⁷ or a relative method^{13,14} (the value of ref 13 superseded a previous value from the same group which was 3 times higher¹⁰). In contrast, the relative rate measurement of ref 15 is 3 times higher than those values. In this relative study, the reference reaction was OH + 2-methyl propene, which has a rate constant ($k = 4.94 \times 10^{-11} \text{ cm}^3 \text{ molecule}^{-1} \text{ s}^{-1}$ at 298 K) 40 times higher than k_1 .¹¹

For the reaction of OH with 4-methyl 2-pentanone, the first temperature-dependent determination of k_4 is reported in the present work. The value at room temperature is in fair agreement with the literature values all obtained using the relative rate method.^{10,13,15–17}

Trends in the OH + Ketones Reaction Rate Constants. The obtained rate constant at 298 K can be compared with the calculated ones using the structure–reactivity relationship (SAR) of Atkinson recently updated.¹⁸ In this method, calculation of H atom abstraction for C–H bonds is based on the estimation of $-\text{CH}_3$, $-\text{CH}_2-$, and $-\text{CH}<$ group rate constants, assuming that the group rate constants depend on the identity of

TABLE 2: Comparison of OH Reaction Rate Coefficients with Previous Work

molecule	<i>T</i> , K	<i>k</i> , ^a 10 ⁻¹² cm ³ molecule ⁻¹ s ⁻¹	<i>A</i> , ^{a,b} 10 ⁻¹² cm ³ molecule ⁻¹ s ⁻¹	<i>E/R</i> , ^{a,b} K	<i>T</i> range, K	technique ^c	ref
CH ₃ C(O)CH ₃	300	≤0.53				RR	10
	300	0.23 ± 0.03				FP-RF	7
	298	0.63 ± 0.09				RR	9
	303	0.27 ± 0.01				RR	8
	296	0.216 ± 0.016	(1.7 ± 0.4)	(600 ± 75)	240–440	FP-RF	6
	1217	8.80 ± 1.32				SH-RA	12
	298	0.184 ± 0.024	(1.25 ± 0.22)	(561 ± 57)	243–372	LP-LIF	this work
CH ₃ C(O)C ₂ H ₅	305	3.5 ± 1.0				RR	15
	300	2.74				RR	10
	295	0.95 ± 0.09				RR	13
	300	1.2 ± 0.2				FP-RF	7
	297	0.97 ± 0.17				RR	14
	296	1.15 ± 0.10	(2.3 ± 1.1)	(170 ± 120)	240–440	FP-RF	6
	298	1.19 ± 0.18	(1.51 ± 0.29)	(60 ± 61)	243–372	LP-LIF	this work
CH ₃ C(O)CH(CH ₃) ₂	298	2.87 ± 0.29	(1.58 ± 0.35)	–(193 ± 65)	253–372	LP-LIF	this work
	305	15 ± 5				RR	15
CH ₃ C(O)CH ₂ CH(CH ₃) ₂	300	13.1				RR	10
	295	13.9 ± 0.4				RR	13
	299	14.3 ± 0.7				RR	16
	297	14.1 ± 0.8				RR	17
	298	12.1 ± 0.9	(0.759 ± 0.126)	–(834 ± 46)	253–372	LP-LIF	this work
	298	10.3 ± 1.0	(1.33 ± 0.63)	–(649 ± 140)	263–372	LP-LIF	this work
	CH ₃ C(O)(CH ₂) ₂ CH(CH ₃) ₂	298	10.3 ± 1.0	(1.33 ± 0.63)	–(649 ± 140)	263–372	LP-LIF

^a Errors are those given by the authors. ^b For our data, the uncertainties for *A* and *E/R* are given by $\Delta A = 2A\sigma_{\ln A}$ and $\Delta E/R = 2\sigma_{E/R}$ for the Arrhenius forms. ^c Key: RR, relative rate; FP-RF, flash photolysis–resonance fluorescence; SH-RA, shock tube–resonance absorption; LP-LIF, laser photolysis–laser induced fluorescence.

substituents attached to the group. At 298 K, the group rate constants are given by $k(\text{CH}_3\text{-X}) = k_{\text{prim}}F(\text{X})$, $k(\text{Y-CH}_2\text{-X}) = k_{\text{sec}}F(\text{X})F(\text{Y})$, $k(\text{Y(Z)CH(X)}) = k_{\text{tert}}F(\text{X})F(\text{Y})F(\text{Z})$, where k_{prim} , k_{sec} , and k_{tert} are the rate constants per $\text{CH}_3\text{-}$, $\text{-CH}_2\text{-}$, >CH- groups and $F(\text{X})$, $F(\text{Y})$, $F(\text{Z})$ are the substituent factors. $k_1\text{--}k_5$ have been calculated using the following parameters at 298 K:¹⁸ $k_{\text{prim}} = 0.136 \times 10^{-12}$, $k_{\text{sec}} = 0.934 \times 10^{-12}$, $k_{\text{tert}} = 1.94 \times 10^{-12}$ (units of $\text{cm}^3 \text{ molecule}^{-1} \text{ s}^{-1}$), $F(\text{-CH}_3) = 1$, $F(\text{-CH}_2\text{-}) = F(\text{-CH<}) = F(\text{>C<}) = 1.23$, $F(\text{>CO}) = 0.75$, $F(\text{-CH}_2\text{C(O)R}) = 3.9$. The experimental and calculated values $k_1\text{--}k_5$ are in pretty fair agreement (the calculated values are in parentheses): $k_1 = 0.18 \pm 0.02$ (0.20), $k_2 = 1.19 \pm 0.18$ (1.33), $k_3 = 2.87 \pm 0.29$ (2.62), $k_4 = 12.1 \pm 0.9$ (8.89), $k_5 = 10.3 \pm 1.0$ (8.17). Units are $10^{-12} \text{ cm}^3 \text{ molecule}^{-1} \text{ s}^{-1}$.

Whereas the present data confirm that k_2 is much higher than k_1 , it is shown from the first determination of k_3 reported in this work that k_4 is also much higher than k_3 . This confirms the activating effect of the >CO group on the CH_x ($x = 1, 2, 3$) group in the β position, first observed by Atkinson et al.¹⁶ This is reflected in the substituent factor, $F(\text{-CH}_2\text{C(O)R}) = 3.9$,¹⁸ which is much higher than $F(\text{-CH}_2\text{-}) = 1.23$. Besides, our determination of k_5 , which is lower than k_4 , indicates that the -CH< group in the γ position of the >CO group is less reactive than that in the β position. A similar result has been previously obtained for the -CH_3 group from the study of OH reaction with aliphatic ketones.⁶ Our data indicate that $F(\text{-(CH}_2)_2\text{-C(O)R}) < F(\text{-CH}_2\text{-C(O)R}) = 3.9$, but they do not tell if $F(\text{-(CH}_2)_2\text{-C(O)R})$ is equal or higher than $F(\text{-CH}_2\text{-}) = 1.23$. In our SAR calculation of k_5 , it is assumed that $F(\text{-(CH}_2)_2\text{-C(O)R}) = F(\text{-CH}_2\text{-})$.

The rate constants of OH reaction with the studied ketones $\text{CH}_3\text{C(O)R}$ can also be calculated by assuming that the reactivities of the CH_3 and R groups on either side of the carbonyl group, as suggested for reactions of OH with aliphatic ketones,⁶ are independent and additive. Thus $k(\text{CH}_3\text{C(O)R}) = k(\text{CH}_3) + k(\text{R})$. Using $k(\text{CH}_3) = k_1/2 = 0.10 \times 10^{-12} \text{ cm}^3 \text{ molecule}^{-1} \text{ s}^{-1}$ at 298 K, the new values of k_3 and k_5 reported in this work provide the following new group rate constants at 298 K: $k(i\text{-C}_3\text{H}_7) = 2.7 \times 10^{-12}$ and $k(i\text{-C}_5\text{H}_{11}) = 10.2 \times 10^{-12}$

TABLE 3: Reactivity of Alkyl Groups R in Ketones at 298 K

alkyl group R	$10^{12} \times k(\text{R})$ $\text{cm}^3 \text{ molecule}^{-1} \text{ s}^{-1}$
CH ₃ –	0.10 ^a
<i>n</i> -C ₂ H ₅ –	1.0 ^b
<i>n</i> -C ₃ H ₇ –	3.9 ^c
	4.9 ^d
iso-C ₃ H ₇ –	2.7 ^e
<i>n</i> -C ₄ H ₉ –	9.0 ^f
	6.5 ^g
iso-C ₄ H ₉ –	13.7 ^h
tert-C ₄ H ₉ –	1.1 ⁱ
<i>n</i> -C ₅ H ₁₁ –	8.8 ^j
iso-C ₅ H ₁₁ –	10.2 ^k

^a From acetone (average value from [ref 6, this work]). ^b From 2-butanone (average value from [ref 6, this work]). ^c From 2-pentanone [ref 6]. ^d From 2-pentanone [refs 16, 19]. ^e From 3-methyl 2-butanone [this work] and 2,4-dimethyl 3-pentanone [ref 16]. ^f From 2-hexanone [refs 16, 19]. ^g From 2-hexanone [6]. ^h From 4-methyl 2-pentanone (average value from refs 10, 13, 15–17 and this work). ⁱ From 3,3-dimethyl 2-butanone [ref 6]. ^j From 2-heptanone [ref 6]. ^k From 5-methyl 2-hexanone [this work].

$\text{cm}^3 \text{ molecule}^{-1} \text{ s}^{-1}$. These values complement those previously obtained for aliphatic R groups (Table 3). These values may be used to estimate rate constants for OH reaction with ketones $\text{RC(O)R}'$, R and R' being one of these groups.

From the existing rate constant data at 298 K for reaction of OH with ketones [refs 6, 16, 19, and this work], it is possible to derive group rate constants for each CH_x ($x = 1, 2, 3$) group of the ketones as a function of their position relative to the carbonyl group. The data that are reported in Table 4 are derived from the rate constant of OH reaction with the following ketones: $k(\text{CH}_3)_\alpha$ from acetone [refs 6, 16, and this work], $k(\text{CH}_3)_\beta$ from 3,3-dimethyl 2-butanone [ref 60], $k(\text{CH}_2)_\alpha$ from 2-butanone [refs 6, 16, and this work], $k(\text{CH}_2)_\beta$ from 2-pentanone [refs 6, 16, 19], $k(\text{CH}_2)_\gamma$ from 2-hexanone [refs 6, 16, 19], $k(\text{CH})_\alpha$ from 3-methyl 2-butanone [this work] and 2,4-dimethyl 3-pentanone [ref 16], $k(\text{CH})_\beta$ from 4-methyl 2-pentanone [refs 6, 16, and this work], $k(\text{CH})_\gamma$ from 5-methyl

TABLE 4: Rate Constant for Each Group CH_x ($x = 1, 2, 3$) in Ketones at 298 K^{a,b}

CH_x group	position α	position β	position γ	position $\geq \delta$
CH_3	0.10	0.37	0.17	0.17
CH_2	0.7	3.5	3.5	1.4
CH	2.0	12.7	5.6	2.4

^a See text. ^b Rate constant units are $10^{-12} \text{ cm}^3 \text{ molecule}^{-1} \text{ s}^{-1}$.

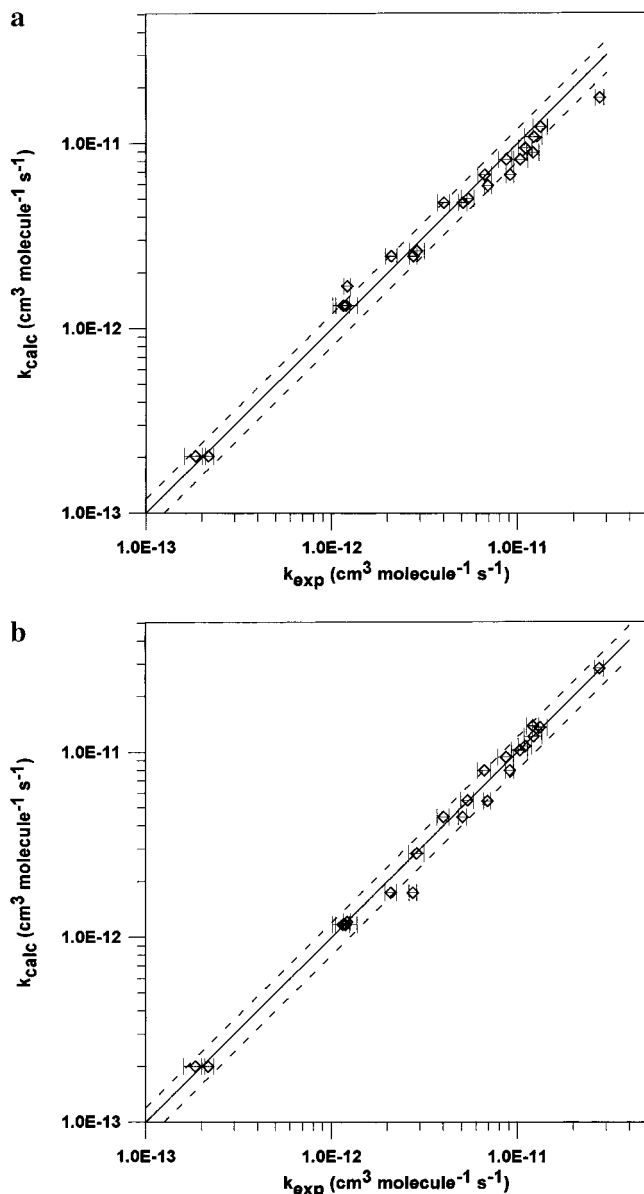


Figure 3. Comparison of the experimental, k_{exp} , and calculated, k_{calc} , rate constants at room temperature for OH reaction with some ketones. Experimental data are from this laboratory [this work], from refs 6, 16, and 19. The dashed lines correspond to a departure of 20% from the best fit (solid line). (a) The SAR is used to calculate the rate coefficients and the substituent factors are $F(-\text{CH}_2-\text{C}(\text{O})\text{R}) = 3.9$ and $F(-\text{C}(\text{O})\text{R}) = 0.75$.¹⁸ (b) The rate coefficients are calculated by adding the rate coefficients of each CH_x group, which are given in Table 4.

2-hexanone [this work]. For CH_x ($x = 1, 2, 3$) groups in the δ position and beyond and also CH_3 in the γ position, $k(\text{CH}_x)$ are taken from the SAR calculation for alkanes.¹⁸ The reactivities of these groups are considered not to be influenced by the carbonyl group. The data of Table 4 lead to the following ratios: $k(\text{CH}_3)_\beta/k(\text{CH}_3)_\alpha = 3.70$, $k(\text{CH}_2)_\beta/k(\text{CH}_2)_\alpha = 5.57$, and $k(\text{CH})_\beta/k(\text{CH})_\alpha = 6.35$, which should be the same and equal to $F(-\text{CH}_2\text{C}(\text{O})\text{R})/F(-\text{C}(\text{O})\text{R}) = 5.2$ given by the SAR method.¹⁸

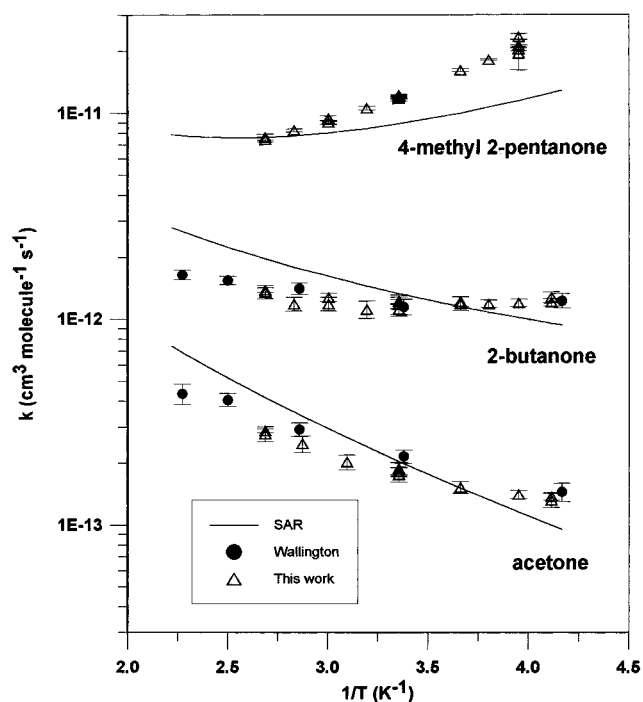


Figure 4. Comparison between the experimental rate coefficients [this work, ref 6] and the calculated ones by SAR¹⁸ vs temperature.

Similarly, the ratios $k(\text{CH}_2)_\beta/k(\text{CH}_2)_\gamma$ and $k(\text{CH})_\beta/k(\text{CH})_\gamma$ are respectively 1 and 2.4, and not equal, as expected from the SAR parameters.

The comparison of the experimental rate constant for the studied OH + ketone reactions [refs 6, 16, 19 and this work] with the calculated ones is given in Figure 3. The calculations have been made using the SAR method (Figure 3a) and the $k(\text{CH}_x)$ additivity method based on the data of Table 4 (Figure 3b). Although the correlation is good with the SAR method, it appears to be slightly better with the $k(\text{CH}_x)$ additivity method. In both methods the calculated and experimental rate constants agree within $\pm 20\%$.

Temperature Dependence of the OH + Ketone Reaction Rate Constants. This work reports the first temperature dependence measurements of k_3 , k_4 , and k_5 and the second ones for k_1 and k_2 . The data reported in Table 2 and Figure 4 show a good agreement with the previous measurement for k_1 and k_2 .⁶ The positive dependence observed for k_1 (OH + $\text{CH}_3\text{C}(\text{O})\text{CH}_3$) is consistent with the similar temperature dependence observed for rate constant of oxygenated compounds containing only CH_3 groups (CH_3OCH_3 , $\text{CH}_3\text{OC}(\text{CH}_3)_3$, $(\text{CH}_3)_3\text{COH}$, $\text{CH}_3\text{C}(\text{O})\text{OCH}_3$, $\text{CH}_3\text{C}(\text{O})\text{OC}(\text{CH}_3)_3$, $\text{HC}(\text{O})\text{OCH}_3$, $\text{HC}(\text{O})\text{OC}(\text{CH}_3)_3$).^{4,20-23}

The temperature dependences of k_2 and k_3 are near zero, whereas they are significantly negative for k_4 and k_5 . 2-Butanone (k_2), 3-methyl 2-butanone (k_3), 4-methyl 2-pentanone (k_4), and 5-methyl 2-hexanone (k_5) all contain CH or CH_2 groups. However, the temperature dependences of k_2 and k_3 can be explained by the fact that 2-butanone (k_2) and 3-methyl 2-butanone (k_3) contain only a CH_2 group and a CH group, respectively, in the α position of the carbonyl group and are deactivated.

The pronounced negative temperature dependences of k_4 and k_5 are consistent with the ones already observed for other oxygenated compounds containing CH or CH_2 groups not deactivated. The SAR calculated values of k_1 , k_2 , and k_4 as a function of temperature are also reported in Figure 4. Some differences with the experimental plots are observed, especially

in the shape of the curves, showing the need of experimental temperature dependence studies in the development of structure–reactivity relationships. Yet, the negative temperature dependence of k_4 and k_5 may indicate the occurrence of an alternative channel in parallel to the direct H atom transfer considered in SAR, as already suggested for OH + ketone reaction.⁶ In such a case the SAR parameters would not have a physical basis but would be only fitting parameters.

Atmospheric Implication. Concerning the atmospheric implication, the rate constant data obtained in the present study contribute to a better definition of the tropospheric lifetimes of the studied ketones which react predominantly with the OH radical. With a typical tropospheric OH concentration of 1×10^6 molecule cm^{-3} the following tropospheric lifetimes toward OH reaction ($\tau = 1/k_1[\text{OH}]$) are estimated: 63 days, 9.7 days, 4.0 days, 23 h, and 27 h for acetone, 2-butanone, 3-methyl 2-butanone, 4-methyl 2-pentanone, and 5-methyl 2-hexanone, respectively. These lifetimes do not take into account loss of the species by photolysis. However, photolysis could contribute significantly to the atmospheric fate of these carbonyl compounds. In particular, it has been shown that for acetone, which reacts rather slowly with OH, photochemistry provides an important pathway in storing NO_x as peroxyacetyl nitrate (PAN) and it is a significant source of HO_x ($\text{OH} + \text{HO}_2$) in the upper troposphere.^{24,25}

Acknowledgment. We thank the French Ministry of Environment through the program Primequal/Predit and the European Commission for support.

References and Notes

- (1) Handon J. D. *Chem. Eng. News* **1997**, 22–23, June 9.
- (2) Atkinson, R. *J. Phys. Chem. Ref. Data* **1997**, 26 (2), 215–290.

- (3) Mellouki, A.; Téton, S.; Laverdet, G.; Quilgars, A.; Le Bras, G. *J. Chim. Phys.* **1994**, 91, 473–487.
- (4) Mellouki, A.; Téton, S.; Le Bras, G. *Int. J. Chem. Kinet.* **1995**, 27, 791–805.
- (5) Martinez, R. D.; Buitrago, A. A.; Howell, N. W.; Hearn, C. H.; Joens, J. A. *Atmos. Environ.* **1992**, 26A, 785–792.
- (6) Wallington, T. J.; Kurylo, M. J. *J. Phys. Chem.* **1987**, 91, 5050–5054.
- (7) Zetzsch, C., 7th Int. Symp. on Gas Kinetics; University Göttingen, W. Germany, August 23–28, 1982; p 73.
- (8) Kerr, J. A.; Stocker, D. W. *J. Atmos. Chem.* **1986**, 4, 253–262.
- (9) Chiorboli, C.; Bignozzi, C. A.; Maldotti, A.; Giardini, P. F.; Rossi, A.; Carassiti, V. *Int. J. Chem. Kinet.* **1983**, 15, 579–586.
- (10) Cox, R. A.; Derwent, R. G.; Williams, M. R. *Environ. Sci. Technol.* **1980**, 14, 57.
- (11) Atkinson, R. *J. Phys. Chem. Ref. Data*, Monograph 2, **1994**.
- (12) Bott, J. F.; Cohen, N. *Int. J. Chem. Kinet.* **1991**, 23, 1017–1033.
- (13) Cox, R. A.; Patrick, K. F.; Chant, S. A. *Environ. Sci. Technol.* **1981**, 15, 587.
- (14) Edney, E. O.; Kleindienst, T. E.; Corse, E. W. *Int. J. Chem. Kinet.* **1986**, 18, 1355–1371.
- (15) Winer, A. M.; Lloyd, A. C.; Darnall, K. R.; Pitts, J. N., Jr. *J. Phys. Chem.* **1976**, 80, 1635.
- (16) Atkinson, R.; Aschmann, S. M.; Carter, W. P. L.; Pitts, J. N., Jr. *Int. J. Chem. Kinet.* **1982**, 14, 839–847.
- (17) O’rji, L. N.; Stone, D. A. *Int. J. Chem. Kinet.* **1992**, 24, 703–710.
- (18) Kwok, E. S. C.; Atkinson, R. *Atmos. Environ.* **1995**, 29, 1685–1695.
- (19) Atkinson, R.; Aschmann, S. M. *J. Phys. Chem.* **1988**, 92, 4008.
- (20) Téton, S.; Mellouki, A.; Le Bras, G.; Sidebottom, H. *Int. J. Chem. Kinet.* **1996**, 28, 291–297.
- (21) El Boudali, A.; Le Calvé, S.; Le Bras, G.; Mellouki, A. *J. Phys. Chem.* **1996**, 100, 12364–12368.
- (22) Le Calvé, S.; Le Bras, G.; Mellouki, A. *Int. J. Chem. Kinet.* **1997**, 683–688.
- (23) Le Calvé, S.; Le Bras, G.; Mellouki, A. *J. Phys. Chem.* **1997**, 101, 5489–5493.
- (24) Singh, H. B.; Kanakidou, M.; Crutzen, P. J.; Jacob, D. J. *Nature* **1995**, 378, 50–54.
- (25) McKeen, S. A.; Gierczak, T.; Burkholder, J. B.; Wennberg, P. O.; Hanisco, T. F.; Keim, E. R.; Gao, R.-S.; Liu, S. C.; Ravishankara, A. R.; Fahey, D. W. *Geophys. Res. Lett.* **1997**, 24, 3177–3180.